

Femtosecond surface plasmon pulse propagation

Zsolt L. Sámson,* Peter Horak, Kevin F. MacDonald, and Nikolay I. Zheludev

Optoelectronics Research Centre, University of Southampton, Highfield, Southampton SO17 1BJ, UK

*Corresponding author: zls@orc.soton.ac.uk

Received September 28, 2010; revised December 6, 2010; accepted December 14, 2010;
posted December 20, 2010 (Doc. ID 135829); published January 13, 2011

We analyze ultrafast surface plasmon-polariton pulse reshaping effects and nonlinear propagation modes for metal/dielectric plasmon waveguides. It is found that group velocity and loss dispersion effects can substantially modify both pulse duration (broadening/narrowing) and intensity decay (acceleration/retardation) by as much as several tens of percentage points in the short-pulse regime and that metallic nonlinearities alone may support soliton, self-focusing, and self-compressing modes. © 2011 Optical Society of America

OCIS codes: 240.6680, 320.7120, 320.5540, 190.5530.

Much interest in surface plasmon-polaritons (SPPs) is derived from the possibility that plasmonic technologies offer to bridge the gap between today's fast, high-bandwidth (but diffraction-limited) photonic and nanoscale (but speed- and bandwidth-limited) electronic systems [1,2]. With such applications in mind, there is growing interest in ultrafast and nonlinear plasmonic phenomena, from active modulation to "coherent control" and soliton propagation [3–10], relevant to high-frequency plasmonic data transport and signal manipulation. It is well known that short optical pulses are distorted as they travel through dispersive and/or absorbing media, and one may anticipate that such effects will be more pronounced in plasmonic systems, which by their very nature must contain lossy, dispersive metals. Here we analyze the reshaping of femtosecond SPP pulses propagating on planar metal/dielectric waveguides and consider the implications for future linear and nonlinear ultrafast plasmonic device applications.

Dispersive media are characterized by frequency (wavelength)-dependent values of refractive index, absorption coefficient, group velocity, etc., which are often adequately described by equations such as those of the Drude or Lorentz–Drude [11] models. However, in the present analysis such approximations are found to be entirely unsuitable: Collective oscillator models cannot account for the complex material-specific peculiarities of real media and produce extremely misleading results in the short-pulse regime. We therefore employ experimentally determined optical constants from [12] (metals) and [13] (fused silica) in what follows.

SPPs propagating on an ideally flat metal/dielectric interface (Fig. 1) are characterized by a wavelength-dependent propagation length, $\delta_{\text{SPP}} = 1/(2k''_{\text{SPP}})$, over which the power or intensity of the mode falls to 1/e of its initial value [14]. Here, k''_{SPP} is the imaginary part of the complex SPP wave vector $k_{\text{SPP}} = k_0 n_{\text{SPP}}$, where $n_{\text{SPP}} = \sqrt{(\epsilon_d \epsilon_m)/(\epsilon_d + \epsilon_m)}$ is the SPP refractive index and k_0 , ϵ_d , and ϵ_m are the free-space wave vector and the complex relative permittivities of the dielectric and metal waveguide components, respectively.

In a plasmonic waveguide, the dispersion of both the real and imaginary parts of n_{SPP} , i.e., both group-velocity dispersion (GVD) and loss dispersion (LD), will contribute substantially to the reshaping of short pulses. It is therefore informative in the first instance to analyze these effects separately: Consider the propagation of

an SPP pulse with a Gaussian field amplitude profile $A(x, t)$ at the input to a planar SPP waveguide (i.e., at $x = 0$ in Fig. 1), given by $A(0, t) = \exp(-t^2/\tau_0^2)$, where τ_0 is the 1/e half-width [15]. To isolate the impact of GVD, one must Fourier transform this profile and in the wavelength (frequency) domain apply a multiplication factor, $M'_i = \exp[ik'_{\text{SPP}}(\lambda_i)x] = \exp[ik_0 n'_{\text{SPP}}(\lambda_i)x]$, where n'_{SPP} is the real part of n_{SPP} that adjusts each component, λ_i (Fig. 1), for dispersive broadening as it travels a distance, x (in the present case, a distance of one propagation length for the center wavelength, λ_0), before executing the inverse Fourier transform to recover the temporal amplitude profile of the output pulse. Intensity $I = |A|^2$.

Figure 2 shows GVD-induced pulse broadening as a function of input pulse duration and wavelength for an Al/silica SPP waveguide (over a parameter space where deviations of output pulse profile from the input Gaussian are small and confined to the low-intensity fringes of the pulse—see inset). Here, substantial temporal broadening, by a factor of up to 1.3 per propagation length, δ_{SPP} , occurs for the shortest pulses at near-IR wavelengths where both bandwidth and SPP propagation length are relatively large. It should be noted that pulse width is not the only characteristic affected here: If a Gaussian pulse is broadened by a factor of 1.3, conservation of energy dictates that its peak amplitude will fall by a factor of 1.3 even *before* the exponential decay due to losses described by δ_{SPP} is taken into account.

The effects of loss dispersion in the absence of GVD can be analyzed by substituting, in the above procedure,

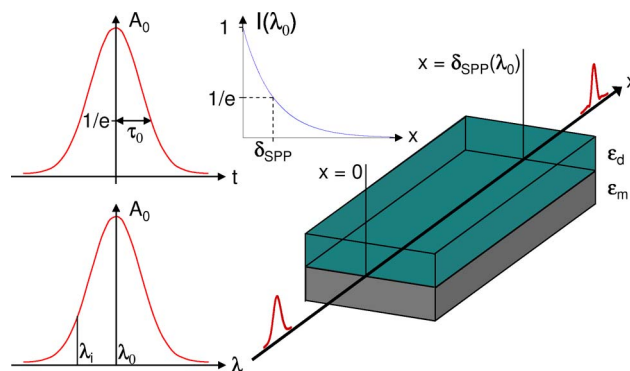


Fig. 1. (Color online) Femtosecond SPP pulse and waveguide parameters: left, Gaussian input pulse amplitude profiles in temporal and spectral domains; right, planar waveguide geometry and exponential intensity decay characteristic.

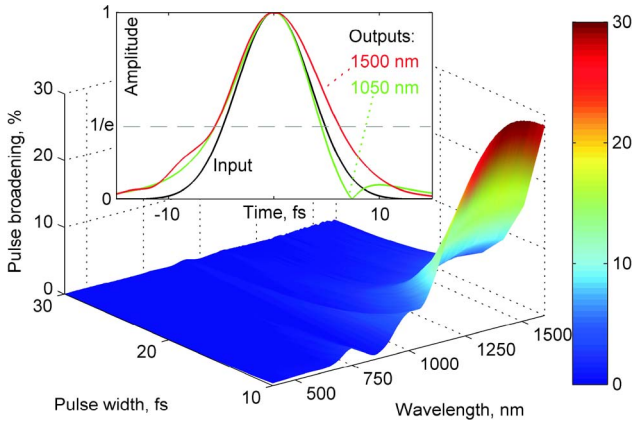


Fig. 2. (Color online) Percentage GVD-induced SPP pulse broadening per propagation length against input pulse width and center wavelength for an Al/SiO₂ waveguide. The inset shows *normalized* 10 fs input (black) and corresponding output pulse profiles at selected wavelengths.

a factor, $M_i'' = \exp[-k_{\text{SPP}}''(\lambda_i)x] = \exp[-x/[2\delta_{\text{SPP}}(\lambda_i)]]$, that adjusts the amplitude of each component, λ_i , according to the losses it experiences during propagation. LD manifests itself most clearly as an acceleration or retardation of SPP pulse decay as shown in Fig. 3, again for an Al/silica waveguide. For many combinations of input pulse duration and center wavelength, the intensity falls, as expected, to $1/e$ of its initial value over a distance, δ_{SPP} . However, output intensities are as much as 28% higher than expected (indicating a decay rate 28% lower than expected) for center wavelengths just above the metal's interband absorption at ~ 800 nm. This implies an LD-induced temporal *narrowing* of pulses at these wavelengths, as opposed to GVD-induced broadening in the same range (again, output pulse profiles deviate little from the input Gaussian—see inset to Fig. 3).

A complete picture of SPP pulse reshaping, accounting for both GVD and LD, through which one may assess the relative merits of different waveguide materials, is obtained by employing a combined multiplication factor, $M_i = M_i' \times M_i'' = \exp[ik_{\text{SPP}}(\lambda_i)x]$. Figure 4 compares Al/

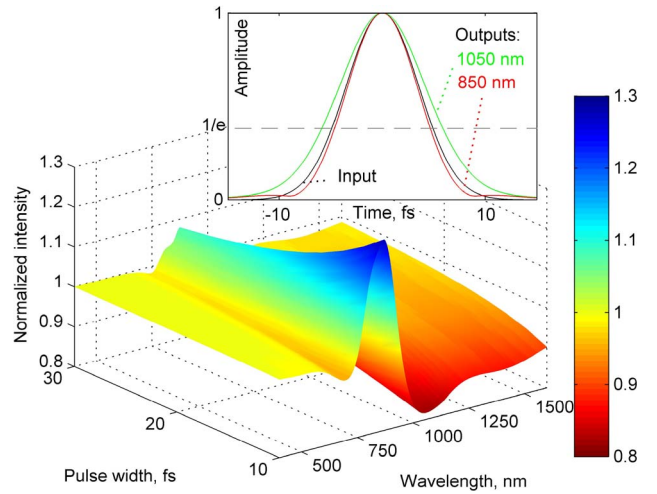


Fig. 3. (Color online) LD-induced variation in SPP pulse output intensity (normalized by a factor, $1/e$) against input pulse duration and center wavelength for an Al/SiO₂ waveguide. The inset shows *normalized* 10 fs input (black) and corresponding output pulse profiles at selected wavelengths.

Ag/, and Au/silica waveguides in terms of broadening and intensity decay for pulses traveling a distance of one propagation length. In the case of Al, the balance between GVD- and LD-induced effects is now seen, with adjacent bands of temporal pulse narrowing (and associated decay retardation) and broadening (with decay acceleration) in the vicinity of the metal's interband absorption resonance. In contrast, Ag presents a largely achromatic picture of minimal reshaping across the visible to near-IR range for all but the shortest pulse durations (< 50 fs). Finally, Au presents a richer pattern of reshaping effects, with a family of pulse broadening and narrowing (enhanced and retarded decay) domains in the visible range and effects that are much more pronounced than in Al or Ag. Importantly, it is found that SPP pulses at 1550 nm (a key telecommunications wavelength) will suffer substantial broadening and accelerated decay.

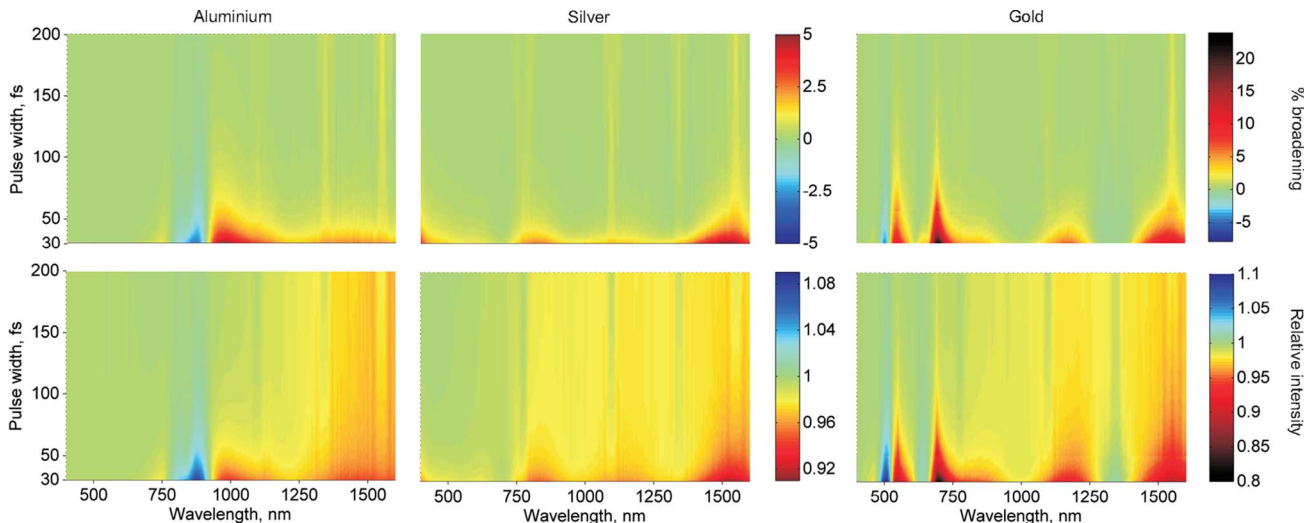


Fig. 4. (Color online) Combined impact of group velocity and loss dispersion on SPP pulse transmission over one propagation length on Al/, Ag/ and Au/silica waveguides: Upper plots show total (GVD- plus LD-induced) percentage pulse broadening; lower plots show normalized output pulse intensity, as functions of input pulse duration and center wavelength.

Although minimal reshaping may be desirable for many short-pulse signal propagation applications, others may benefit from, or indeed rely on, the kind of strong dispersion characteristics indicated in Au or Al SPP waveguides. One is invited by recent reports [4,5,7] to consider nonlinear SPP modes supported by the nonlinearity of the metallic (as opposed to the more conventionally considered dielectric [8–10]) waveguide component: solitons balance nonlinear and dispersive effects to achieve a field profile (temporal or spatial) that does not change during propagation. A preliminary analysis of prospects for achieving a plasmon-soliton may be based on a comparison among SPP propagation length, δ_{SPP} , and characteristic dispersion ($L_{\text{D}} = [4\omega\tau_0^2]/[\lambda|D_\lambda|]$) and nonlinearity ($L_{\text{NL}} = [n_2k_0I_0]^{-1}$) lengths, where ω is the angular frequency, D_λ is GVD given by $[-\lambda/c][d^2n'_{\text{SPP}}/d\lambda^2]$, I_0 is the peak intensity, and n_2 is the nonlinear refractive index [15]. One is seeking to match L_{D} and L_{NL} , ideally at a level far below δ_{SPP} . The first part of this objective can be achieved in a planar Au/silica waveguide with reasonable pulse parameters: 8 fs pulse width, 3 W/ μm^2 peak intensity, and a bulk gold value of the third-order nonlinear susceptibility $\chi^{(3)} = 7.6 \times 10^{-19} \text{ m}^2/\text{V}^2$ [16] give $L_{\text{D}} = L_{\text{NL}} = 4.7 \mu\text{m}$ at a wavelength of 640 nm. However, δ_{SPP} at this wavelength is only 1.9 μm , so fundamental solitons may be difficult to observe. (The situation worsens at longer wavelengths as L_{D} increases much faster than δ_{SPP} .) But the possibility should not be excluded: D_λ may be increased substantially by a *waveguide* dispersion contribution in geometries (e.g., strip, nanowire, and slot waveguides) that also support long-range SPP modes (i.e., provide much larger values of δ_{SPP}). At the same time, $\chi^{(3)}$ may be significantly higher in the near field of a metal surface than in bulk [17]. Further numerical analysis also suggests that higher order solitons, which at increased pulse energies would undergo oscillatory self-focusing and/or temporal compression, may be more readily achieved.

In conclusion, an analytical study of femtosecond SPP pulse reshaping effects in metal/dielectric waveguides finds that group-velocity and loss dispersion can substantially broaden pulses during propagation and accelerate their attenuation, particularly at wavelengths close to interband absorption resonances, with obvious implications for repetition rates and signal-to-noise ratio in many applications. Wavelength bands where one may exploit dispersion-induced temporal pulse narrowing and associated amplitude decay retardation are also

identified, and the pulse reshaping properties of Ag/silica waveguides are found to be remarkably achromatic in the visible to near-IR range. The increasing number of experimental and theoretical studies in ultrafast and nonlinear plasmonics will inform future development of practical technologies in the same way that studies of ultrafast and nonlinear optical phenomena have contributed to the advancement of photonics (especially fiber communications) and, with this in mind, nonlinear SPP propagation modes are considered. Here, our preliminary analysis indicates that soliton, self-focusing, and self-compressing modes supported solely by the nonlinearity of metallic waveguide components may be achieved.

The authors acknowledge the financial support of the Engineering and Physical Sciences Research Council (UK) (EPSRC) and the Royal Society.

References

1. R. Zia, J. A. Schuller, A. Chandran, and M. L. Brongersma, *Mater. Today* **9**, 20 (2006).
2. E. Ozbay, *Science* **311**, 189 (2006).
3. K. F. MacDonald and N. I. Zheludev, *Laser & Photon. Rev.* **4**, 562 (2010).
4. N. Rotenberg, J. N. Caspers, and H. M. van Driel, *Phys. Rev. B* **80**, 245420 (2009).
5. V. V. Temnov, G. Armelles, U. Woggon, D. Guzatov, A. Cebollada, A. Garcia-Martin, J. M. Garcia-Martin, T. Thomay, A. Leitenstorfer, and R. Bratschitsch, *Nat. Photon.* **4**, 107 (2010).
6. M. I. Stockman, D. J. Bergman, and T. Kobayashi, *Phys. Rev. B* **69**, 054202 (2004).
7. J. Renger, R. Quidant, N. van Hulst, S. Palomba, and L. Novotny, *Phys. Rev. Lett.* **103**, 266802 (2009).
8. E. Feigenbaum and M. Orenstein, *Opt. Lett.* **32**, 674 (2007).
9. K. Y. Bliokh, Y. P. Bliokh, and A. Ferrando, *Phys. Rev. A* **79**, 041803 (2009).
10. A. R. Davoyan, I. V. Shadrivov, and Y. S. Kivshar, *Opt. Express* **17**, 21732 (2009).
11. A. D. Rakić, A. B. Djurišić, J. M. Elazar, and M. L. Majewski, *Appl. Opt.* **37**, 5271 (1998).
12. *Handbook of Optical Constants of Solids*, E. D. Palik, ed., (Academic, 1985).
13. I. H. Malitson, *J. Opt. Soc. Am.* **55**, 1205 (1965).
14. W. L. Barnes, *J. Opt. A* **8**, S87 (2006).
15. G. P. Agrawal, *Nonlinear Fiber Optics* (Academic, 2001).
16. R. W. Boyd, *Nonlinear Optics* (Academic, 2008).
17. P. Wang, Y. Lu, L. Tang, J. Zhang, H. Ming, J. Xie, F. H. Ho, H. H. Chang, H. Y. Lin, and D. P. Tsai, *Opt. Commun.* **229**, 425 (2004).